**Loss of EHF promotes the development of treatment-induced neuroendocrine prostate cancer**

Zhi Long[1], Liang Deng[1], Chao Li[1], Qiangrong He[1], Yao He[2], Xiheng Hu[2], Yi Cai[2], Yu Gan[2]

1. Andrology Center, Department of Urology, the Third Xiangya Hospital, Central South University, Changsha, Hunan, P.R. China, 410013;
2. Department of Urology, Xiangya Hospital, Central South University, Changsha, Hunan, P.R. China, 410008;

**Corresponding author:** Yu Gan, M.D.
87 Xiang Road, Changsha
Hunan, P.R. China, 410008
Tel: +86 15111140206
Email: 148302039@csu.edu.cn

**Disclosure Statement:** The authors have declared that no conflict of interest exists.

**Supplementary Materials**

**I. Antibody Information**

| Antibody | Vendor | Catalogue Number | Application | Dilution |
|---|---|---|---|---|
| AR | Proteintech | 22089-1-AP | WB | 1:1000 |
| EHF/ESE-3 | Proteintech | 67125-1-Ig | WB | 1:1000 |
| | Abcam | Ab272671 | IHC | 1:200 |
| ENO2 | Proteintech | 10149-1-AP | WB | 1:1000 |
| | | | IHC | 1:200 |
| CHGA | Proteintech | 60135-1-Ig | WB | 1:2000 |
| H3K27me3 | Omnimabs | OM256819 | WB | 1:1000 |
| Histone H3 | CST | 4499 | WB | 1:1000 |
| EZH2 | Proteintech | 21800-1-AP | WB | 1:1000 |
| SOX2 | Abcam | Ab97959 | WB | 1:1000 |
| | | | IHC | 1:200 |
| Vinculin | Sigma Aldrich | V9131-2ML | WB | 1:2000 |
| Ki-67 | Genetex | GTX16667 | IHC | 1:100 |
| AR | CST | 5153 | ChIP | 1:100 |
| H3K9Ac | CST | 9649 | ChIP | 1:50 |
| Rabbit IgG | Invitrogen | 10500C | ChIP | 1:50/100 |

**Ⅱ. RNA and Plasmid Information**

| Reagent | Provider | Catalogue # |
|---|---|---|
| ON-TARGETplus Human AR siRNA | Dharmacon | L-003400-00-0005 |
| ON-TARGETplus Human EZH2 siRNA | Dharmacon | L-004218-00-0005 |
| ON-TARGETplus Non-targeting Pool | Dharmacon | D-001810-10-05 |
| TRC Lentiviral Human EHF shRNA | Dharmacon | RHS4533-EG26298 |
| pGL3-Promoter Vector | Promega | E1761 |
| pCMV-hAR | Addgene; pCMV-hAR was a gift from Elizabeth Wilson | 89078 |

**Ⅲ. Primers for qPRC**

| Primer name | Forward Primer Sequence (5'-3') | Reverse Primer Sequence (5'-3') |
|---|---|---|
| CHGA | TAAAGGGGATACCGAGGTGATG | TCGGAGTGTCTCAAAACATTCC |
| ENO2 | CTGTGGTGGAGCAAGAGAAA | ACACCCAGGATGGCATTG |
| PSA | AGTGCGAGAAGCATTCCCAAC | CCAGCAAGATCACGCTTTTGTT |
| SLIT2 | CGGAGCAGCAAGCTAAAGAA | GCGACAGGGACAGCATCT |

| | | |
|---|---|---|
| DAB2IP | CTGAGCGGGATAAGTGGATGG | AAACATTGTCCGTCTTGAGCTT |
| ADRB2 | TTCTTGCTGGCACCCAATA | GCCAGGACGATGAGAGACAT |
| GAPDH | GGACCTGACCTGCCGTCTAGAA | GGTGTCGCTGTTGAAGTCAGAG |
| ARE1 (ChIP-Seq) | GAAGCCTGGCATGTTGTACTTG | GGTAGGAACAATTGGAGGGAAGT |
| ARE2 (ChIP-Seq) | TGGAGAACTGGCCCATATTGTT | TGAACCAGTGCCAAATCTGTCT |
| PSA (ChIP-Seq) | CCTAGATGAAGTCTCCATGAGCTACA | GGGAGGGAGAGCTAGCACTTG |

## IV. Supplementary Figures

### Supplementary Figure 1

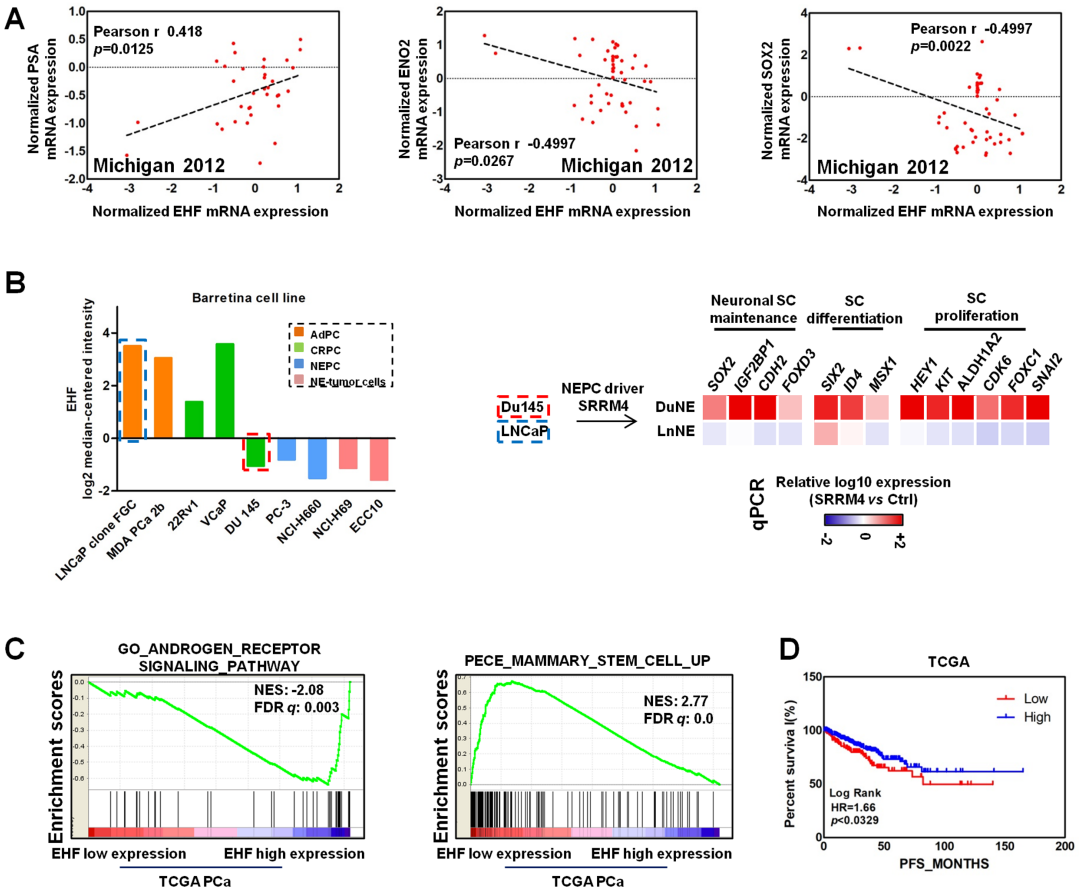


**Figure. S1. (A)** Pearson correlation between EHF and PSA, EHF and ENO2, and EHF and SOX2 expressions was determined using transcriptomic data of Michigan 2012 cohort[1]. **(B)** EHF expression in different cancer cell lines from Barretina *et al.* 2016[2]. Results are presented as mean ± SD (left). The mRNA expression of the genes with functions on neuronal stem cell maintenance, stem cell differentiation and stem cell proliferation in the SRRM4-overexpressing DU145 and LNCaP cells was compared to that of their respective control cells via qPCR. Heat maps represent the relative fold change in log10. **(C)** GSEA analysis indicated that PCa tumors with low EHF expression in TCGA clinical prostate cancer cohort[3] had similarcharacteristics with t-NEPC in alleviating the dependency on AR signaling and gaining stem-cell features. **(D)** Kaplan-Meier analysis indicated that PCa tumors with low EHF

expression had a poor overall survival. Note: AdPC, prostate adenocarcinoma; CRPC, castration-resistant prostate cancer; NEPC, neuroendocrine prostate cancer; NE, neuroendocrine; SC, stem cell; PCa, prostate cancer; NES, Normalized enrichment score; FDR, false discovery rate; PFS, progression-free survival; HR, hazard rate.

**Supplementary Figure 2**

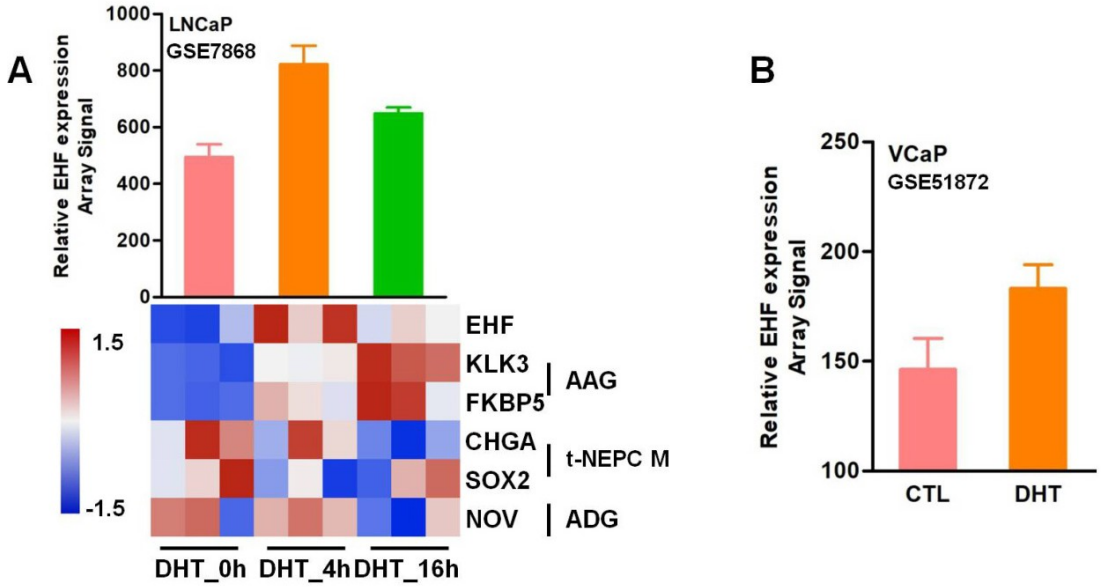


**Figure. S2. (A)** Bar graph showing EHF expression (Top) and heatmap of AR-associated genes including EHF, t-NEPC markers and an androgen-depressed gene in DHT treated LNCaP cells (GSE7868). **(B)** Bar graph showing EHF expression in DHT or ENZ treat VCaP cells (GSE51872). Bar graphs show means ± SD. Note: AAG, AR-associated genes; M, markers; ADG, androgen-depressed gene; AD, androgen deprivation; CTL, control; DHT, double hydrogen testosterone.

**Supplementary Figure 3**

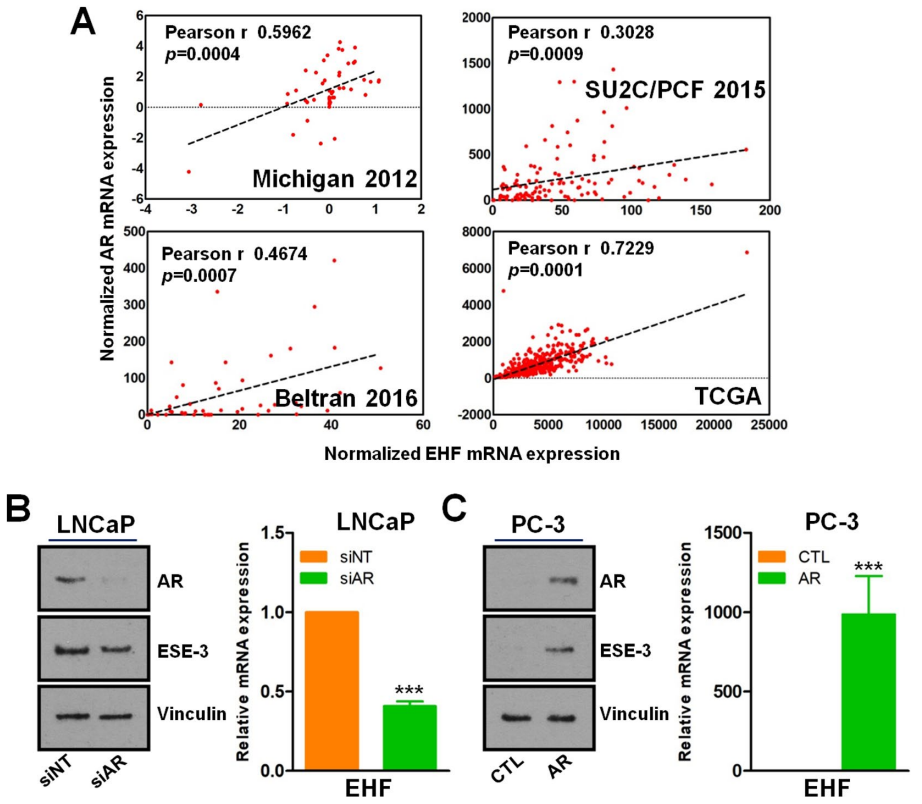


**Figure. S3. (A)** EHF and AR are positive correlated in Michigan 2012[1], SU2C/PCF 2015[4], Beltran 2016[5] and TGCA[3] clinical protate cancer cohort. **(B)** AR and EHF levels in LNCaP cells with/without AR knockdown were measured by qPCR and immunoblotting. **(C)** AR and EHF levels in PC-3 cells with/without AR overexpression were measured by qPCR and immunoblotting. The two-tailed Student's t-test was used to compare results between two groups with *** denoting $p<$ 0.001. Bar graphs show means ± SD. Note: TCGA, the cancer genome atlas; CTL, control; NT, non-target.

**Supplementary Figure 4**

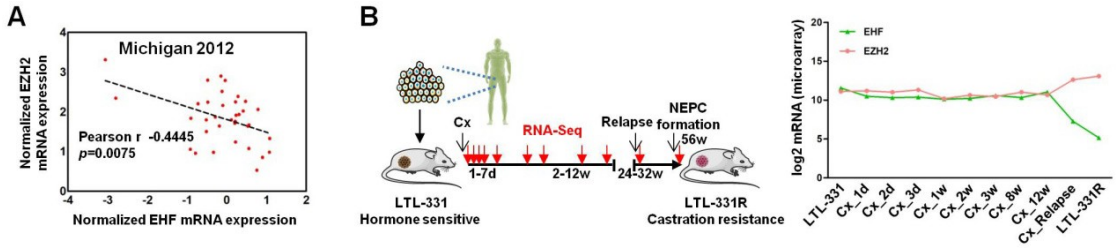


**Figure. S4. (A)** Pearson correlation between EHF and EZH2 was determined using transcriptomic data of Michigan 2012 cohort[1]. **(B)** EHF and EZH2 mRNA expressions during progression of AdPC (LTL-331) to t-NEPC (LTL-331R) by castration surgery to the host mice[6] were plotted. Note: Cx, castration.

**Supplementary Figure 5**

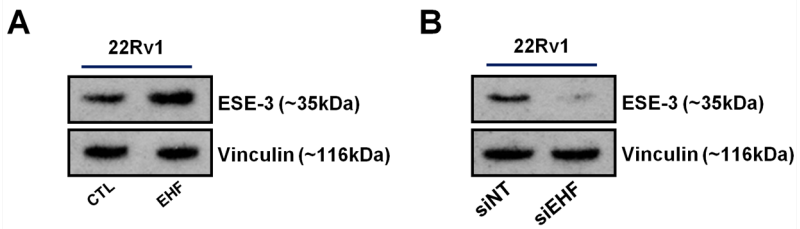


**Figure. S5. (A)** ESE-3 expression level in 22Rv1 cells with/without EHF overexpression was measured by immunoblotting. **(B)** ESE-3 expression level in 22Rv1 cells with/without EHF knockdown was measured by immunoblotting.

**Supplementary Figure 6**

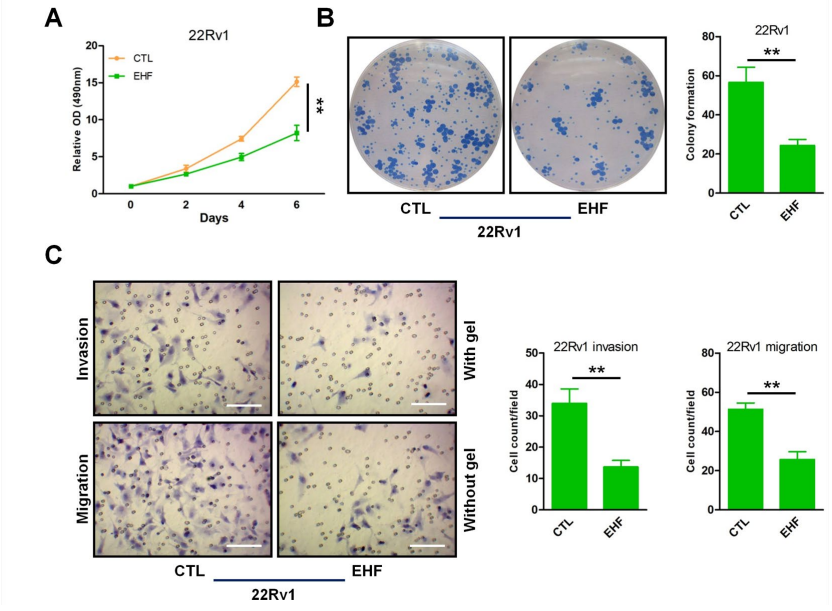


**Figure. S6. (A)** MTS assays measured cell proliferation of 22Rv1 cells with/without EHF

overexpression. **(B)** Same cells as in **A** were used to perform colony formation assays. Representative images are shown. **(C)** Same cells as in **A** were used to perform cell invasion and migration assays in transwell chambers with/without matrigel coated. Representative images are shown. Scale bar 100μm. Two-tailed Student's t-test was used to compare results between two groups with ** denoting $p< 0.01$. Experiments were performed with three biologically independent samples. Bar graphs show means ± SD. Note: OD, optical density.

**Supplementary Figure 7**

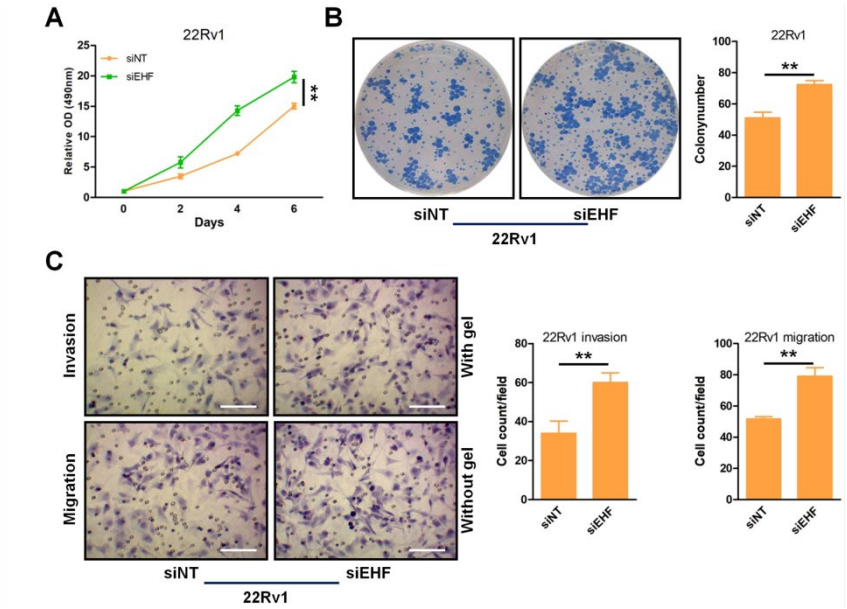


**Figure. S7. (A)** MTS assays measured cell proliferation of 22Rv1 cells with/without EHF knockdown. **(B)** Same cells as in **A** were used to perform colony formation assays. Representative images are shown. **(C)** Same cells as in **A** were used to perform cell invasion and migration assays in transwell chambers with/without matrigel coated. Representative images are shown. Scale bar 100μm. Two-tailed Student's t-test was used to compare results between two groups with ** denoting $p< 0.01$. Experiments were performed with three biologically independent samples. Bar graphs show means ± SD. Note: OD, optical density.

## V. References


1. Grasso CS*, et al.* The mutational landscape of lethal castration-resistant prostate cancer. *Nature* **487**, 239-243 (2012).
2. Barretina J*, et al.* The Cancer Cell Line Encyclopedia enables predictive modelling of anticancer drug sensitivity. *Nature* **483**, 603-607 (2012).
3. Cancer Genome Atlas Research N. The Molecular Taxonomy of Primary Prostate Cancer. *Cell* **163**, 1011-1025 (2015).
4. Robinson D*, et al.* Integrative Clinical Genomics of Advanced Prostate Cancer. *Cell* **162**, 454 (2015).
5. Beltran H*, et al.* Divergent clonal evolution of castration-resistant neuroendocrine prostate cancer. *Nature medicine* **22**, 298-305 (2016).
6. Lin D*, et al.* High fidelity patient-derived xenografts for accelerating prostate cancer discovery and drug development. *Cancer research* **74**, 1272-1283 (2014).